NEW TECHNOLOGIES FOR DESIGN
AND PROCESSING OF MATERIALS

The Formation of the Surface Layers of a VT6 Titanium Alloy by Ion Beam Mixing of Carbon Nanofilms

V. L. Vorobyov[a], *, A. A. Kolotov[a], **, A. L. Ulyanov[a], *, F. Z. Gilmutdinov[a], ****,**
P. V. Bykov[a], S. G. Bystrov [a], ***, and V. Ya. Bayankin[a]**

[a]Udmurt Federal Research Center, Ural Branch, Russian Academy of Sciences, Izhevsk, 426067 Russia
*e-mail: Vasily_L.84@mail.ru
**e-mail: less@udman.ru
***e-mail: ulyanov@ftiudm.ru
****e-mail: gilmutdinov_f@mail.ru
*****e-mail: bystrov.sg@mail.ru

Abstract—The influence of ion beam mixing of carbon on the surface morphology, chemical composition, atomic structure, and microhardness of the surface layers of samples of a VT6 titanium alloy is investigated. It is found that conditions for the formation of titanium carbides are created in the transition layer of the film/substrate system during ion beam mixing. The formation of titanium carbides with both stoichiometric and nonstoichiometric ratios of the components occurs. The concentration of titanium carbides increases with the increase in the irradiation dose and reaches 20 at % at a dose of 4×10^{17} ion/cm^2. The mixing manifests itself in the mutual penetration of carbon atoms into the target and target atoms, mainly titanium, into the film. However, a thin surface layer with a depth of about 20 nm which is mainly composed of carbon atoms remains. It is shown that, in this layer, carbon atoms are in a disordered state with both sp^2 and sp^3 hybridization of the C−C bonds. The formation of titanium carbides in the transition layer and the disordered structure of carbon on the surface of the film during ion beam mixing determines the hardening of the surface layer, and as a result, an increase in the microhardness of the samples by 100% or more occurs. It is shown that the growth in the microhardness is associated with the layer formed as a result of mixing rather than the influence of irradiation on the titanium alloy substrate.

INTRODUCTION

Films and coatings on the basis of transition metal carbides and nitrides are widely used in mechanical engineering, microelectronics, medicine, and other fields for increasing the strength characteristics of materials, protection of the surface against corrosion, improvement of the design of goods, etc. [1, 2]. Methods of ion beam treatment are a promising method for the formation of coatings and films with predefined properties [3]. In particular, the action of a beam of high-energy ions on the nanolayers of a doping substance preliminarily applied to the surface of a target using a magnetron technique makes it possible to form nano-sized coatings with high adhesion to the substrate [4]. Despite the research in this direction, the processes of formation of nanosized carbon and carbon−carbide coatings on metallic surfaces upon ion beam mixing are inadequately studied.

The aim of this work is to study the morphology of the surface, chemical and phase composition, inter-atomic chemical bonds, atomic structure, and mechanical properties (microhardness) of carbon films formed on the surface of VT6 titanium alloy via magnetron sputtering followed by ion beam treatment with a beam of high-energy Ar$^+$ ions.

EXPERIMENTAL

Samples of VT6 titanium alloy which were plates with a size of 10 × 10 mm and a thickness of 2 mm were studied in this work. The surface of the samples was subjected to mechanical sanding and filing, after which it was purified in organic solvents using ultrasound.

Prior to applying a carbon film, recrystallization annealing of the samples at 800°C for 1 h in high vacuum of ~10^{-5} Pa and "cleaning" of the surface with argon ions with the energy of 1.8 keV, beam current of 100 mA, and time of etching of 20 min were performed. The sputtering of the carbon film was per-

Table 1. Values of the roughness parameter R_a of the surface of the samples in the initial state, after the sputtering of a carbon film, and after ion beam mixing

Sample	Roughness parameter, R_a, nm	Mean square deviation, MSD, nm
VT6	9.3	2.6
C/VT6	12.0	3.4
$Ar_1^+ \rightarrow$ C/VT6	11.7	2.8
$Ar_2^+ \rightarrow$ C/VT6	10.3	1.4

formed via a magnetron technique with the use of graphite targets on a Katod-1M unit in an argon atmosphere at a constant current and a temperature of the support of 523 K. The thickness of the sputtered film was 60−70 nm.

Ion beam mixing of the carbon films was performed by means of irradiation with Ar^+ ions in a repetitively pulsed mode (100 Hz, 1 ms) with the energy of the ions of 30 keV, ion current density in the pulse of 3 mA/cm^2, and irradiation doses of 10^{17} and 4×10^{17} ion/cm^2 (these samples are denoted as $Ar_1^+ \rightarrow$ C/VT6 and $Ar_2^+ \rightarrow$ C/VT6, respectively). The calculated value of the projective range of Ar^+ ions in graphite at the kinetic energy of ions of 30 keV is ~25 nm [5]. Several samples of the titanium alloy were irradiated with Ar^+ ions with the parameters identical to those used in the case of ion beam mixing with the irradiation dose of 10^{17} ion/cm^2.

The following notation of the samples is used in the work: VT6 is the initial sample, C/VT6 is the sample with a sputtered carbon film, $Ar_1^+ \rightarrow$ C/VT6 and $Ar_2^+ \rightarrow$ C/VT6 are the samples after the mixing of the carbon film with Ar^+ ions with irradiation doses of 10^{17} and 4×10^{17} ion/cm^2, respectively, and $Ar_1^+ \rightarrow$ VT6 is the sample after irradiation with Ar^+ ions with the irradiation dose of 10^{17} ion/cm^2.

The topography of the samples was studied via atomic force microscopy (AFM) on a SOLVER P47 PRO microscope in a contact mode. The arithmetic average roughness (R_a) of the surface was calculated by the images of 12 regions with the base dimensions of 1×1 μm for each sample using the Image Analysis 3.5.0 program.

The microhardness of the samples was measured and calculated according to GOST (State Standard) 2999-75. The measurements were performed using a PMT-3M microhardness tester at indentation loads of 5 and 20 g and duration of the exposure under load of 10 s. The depth of indentation at a load of 5 g was varied within 1.3−2.0 μm, and at a load of 20 g, it was varied within 2.2−3.0 μm. To improve the reliability of the data obtained, at least twenty measurements of

microhardness were performed for each state under study. The results were averaged, and the mean square deviation of the measured values of microhardness was calculated.

The Raman spectra (RS) of the films were obtained on a HORIBA Jobyn Yvon HR800 spectrometer using a helium−neon laser ($\lambda_{ex} = 632.8$ nm) and an objective lens with the magnification of ×100. The diameter of the laser beam was 5 μm and the time of exposure was 5 s.

The chemical composition of the surface layers was studied via X-ray photoelectron spectroscopy (XPS) on a SPECS spectrometer using Mg$K\alpha$ radiation (1253.6 eV). The layerwise elemental analysis was executed by etching the surface with argon ions with the energy of 4 keV and current density of 30 μA/cm^2. At these parameters of the argon ions, the rate of etching of the surface is ~1 nm/min. The experimental data were processed using the CasaXPS software package. The relative error of determination of the concentration of elements was ±3 at % of the value being measured.

The X-ray diffraction studies were performed on a DRON-3M diffractometer in a monochromatized Cu$K\alpha$ radiation. The X-ray phase analysis and the precision measurement of the lattice parameters were performed using the full-profile analysis software package [6]. Here, all the reflections in the angular range 2θ from 20° to 130° were taken into account in the calculation. To determine the grain size and values of microdistortions, a modified Warren−Averbach frequency analysis method with the approximation of the shape of the diffraction line by the Voigt function was used [7]. This method makes it possible to use one reflection of the diffraction patterns of a sample and a reference for the analysis.

RESULTS AND DISCUSSION

The AFM studies of the topography of the surface of the samples give evidence of the fact that neither the sputtering of a carbon film nor its ion beam mixing leads to a change in the roughness parameter R_a of the surface (Table 1). The value of the roughness parameter R_a of the surface of the samples in the initial state is 9.3 nm. After the sputtering of a carbon film and its mixing with Ar^+ ions, the values of the parameter R_a within the mean square deviations (MSDs) do not differ from R_a for the initial surface.

The microhardness was measured at indentation loads of 5 and 20 g. The average value of the microhardness of the samples in the initial state in the case of the measurement with a load of 5 g is ~39 MPa (Fig. 1). In this case, the depth of indentation is 2.0 μm. The sputtering of a carbon film does not lead to a growth in the microhardness of the samples of the titanium alloy (Fig. 1). In turn, ion beam mixing of the carbon film with irradiation doses of 10^{17} and 4×10^{17} ion/cm^2 determines an increase in the microhardness of the
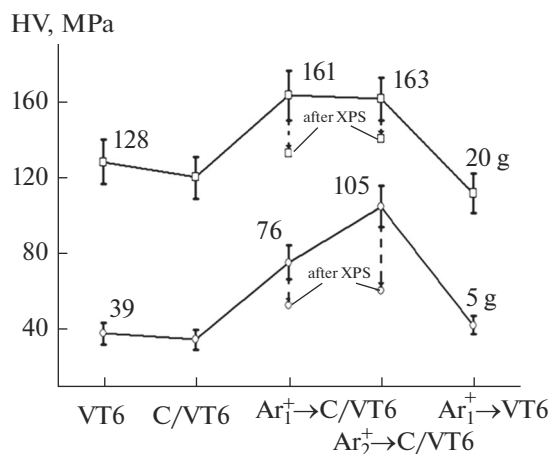
Fig. 1. The microhardness of the surface layers of the samples of VT6 in the initial state (VT6), after deposition of a carbon film (C/VT6), after its ion beam mixing with irradiation doses of 10^{17} ($Ar_1^+ \rightarrow$ C/VT6) and 4×10^{17} ion/cm^2 ($Ar_2^+ \rightarrow$ C/VT6), after implantation of Ar$^+$ ions with a dose of 10^{17} ion/cm^2 ($Ar_1^+ \rightarrow$ VT6), and after XPS studies of the samples with a mixed carbon film.

samples by 100 and 130%, respectively (Fig. 1). The depth of indentation decreases to 1.3 μm. The irradiation of the surface of the titanium alloy without a carbon film with Ar$^+$ ions with the parameters identical to those used in the case of mixing of a carbon film with the irradiation dose of 10^{17} ion/cm^2 does not lead to an increase in the microhardness (Fig. 1). This is evidence of the fact that the growth in the microhardness is determined by the state formed on the surface as a result of the mixing of the carbon film. The performed additional experiment on the measurement of the microhardness of the samples after the "removal" of the mixed layer from their surface by ion etching confirms this assumption. It turned out that the value of the microhardness of the samples decreased and approached the values of the microhardness for the initial sample (Fig. 1, the dotted line). It can be considered that their values do not differ from each other within the error of determination of microhardness. The growth in the microhardness of the samples after ion beam mixing is also confirmed in the case of the measurements with the indentation load of 20 g (Fig. 1). In this case, the value of the microhardness for the samples in the initial state is 128 MPa, and it increases to ~160 MPa after mixing. The depth of indentation varies within 2.2–3.0 μm.

The XPS studies of the surface of the samples revealed that the bombardments with Ar$^+$ ions led to the mixing of the sputtered film with the atoms of the target (Fig. 2). The depth of the carbon-containing surface layer can be conditionally divided to two layers, namely, the first layer predominantly consisting of
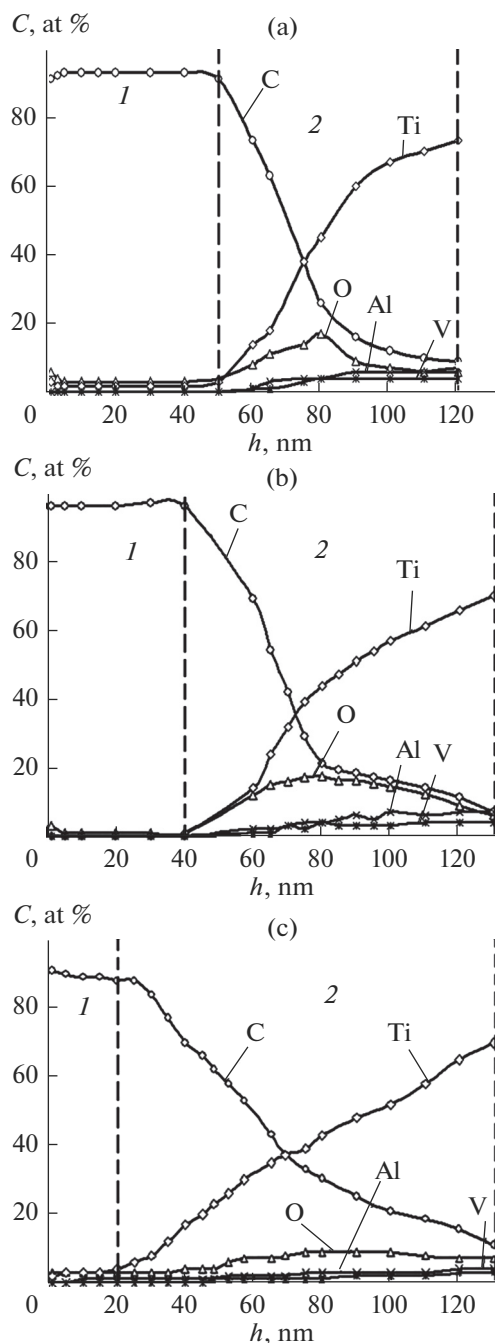

Fig. 2. Distribution of the elements in the surface layers of the samples of the titanium alloy: (a) with a sputtered carbon film and (b, c) after ion beam mixing at irradiation doses of (b) 10^{17} and (c) 4×10^{17} ion/cm^2.

carbon and the second, transition, layer (Fig. 2). The depth from which the concentration of titanium starts increasing and the concentration of carbon starts decreasing can be taken for the beginning of the transition layer. The depth where the concentration of titanium would correspond to its concentration in the bulk can be taken for the end of the transition layer. This value is ~75 at % (Fig. 2a). For the initial film, the
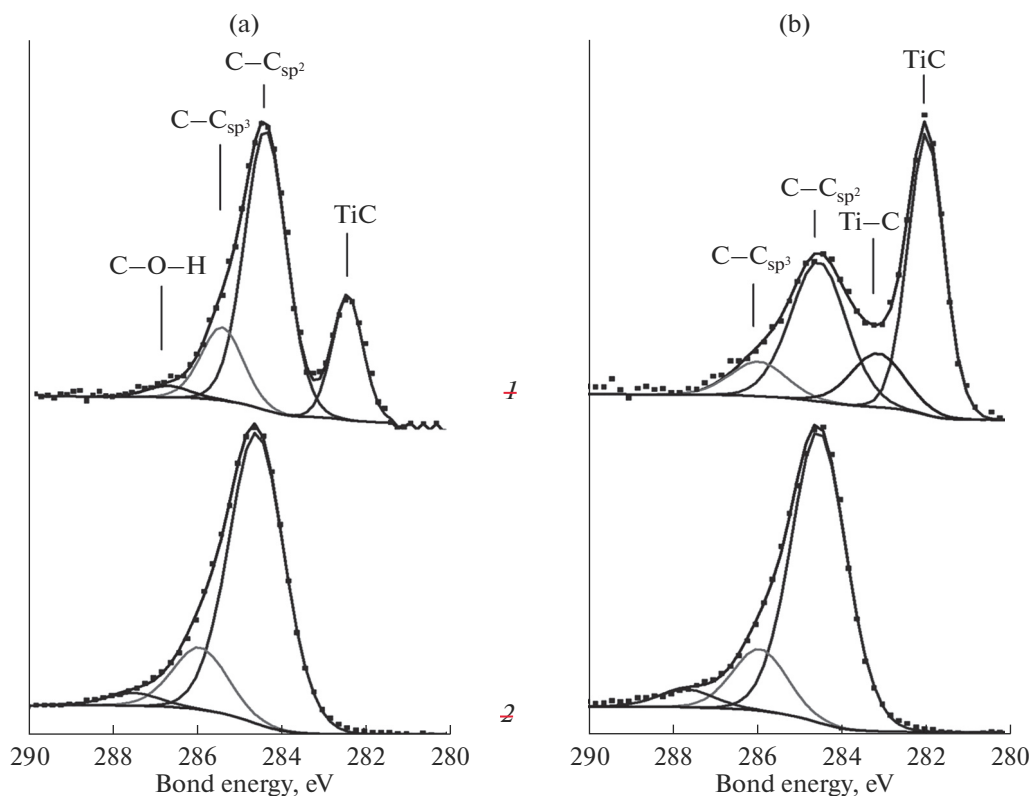
Fig. 3. C1s spectra from the depth of the samples of VT6 of (I) ~30 and (2) ~90 nm: (a) with a sputtered carbon film and (b) after its ion beam mixing with a dose of 10^{17} ion/cm^2.

layer with the predominant concentration of carbon is about 50 nm, and the transition layer is about 70 nm (Fig. 2a). As a result of the mixing, the thickness of the first layer decreases, which can be due to the partial sputtering of carbon upon ion bombardment. In turn, the depth of the transition layer increases and is more than 100 nm in the case of ion beam mixing with the dose of 4×10^{17} ion/cm^2 (Fig. 2c). The increase in the depth of the transition layer is determined by the mutual penetration of the carbon atoms into the target and atoms of the target (mainly titanium atoms) into the film upon ion bombardment.

The XPS spectra of the elements in the surface layers of the samples were analyzed; the C1s XPS spectra turned out to be the most informative. The decompo-

Table 2. Change in the CSRs of the samples

Sample	CSR, nm
VT6	48 ± 2
C/VT6	48 ± 2
$Ar_1^+ \rightarrow$ C/VT6	35 ± 2
$Ar_2^+ \rightarrow$ C/VT6	36 ± 2
$Ar_1^+ \rightarrow$ VT6	38 ± 2

sition of the C1s spectra into components made it possible to distinguish three states of carbon in the first layer of the initial film (Fig. 3a, spectrum I). The first state is the form of carbon with the bond energy of 284.6 eV which is characterized by the sp^2 type of hybridization of the C–C bonds. The second peak with the bond energy of 286 eV can be interpreted as carbon with the sp^3 type of hybridization of the C–C bonds. The third (weak) peak in the region of high bond energies is the form of carbon with C–O–H bonds. It is seen from the presented decomposition of the C1s spectrum that carbon atoms in the first layer of the initial film as well as after ion beam mixing predominantly are in the C–C bonds with the sp^2 type of hybridization of the electrons. The C1s spectrum of carbon in the film after mixing in the layer with the predominant concentration of carbon is also represented by these components (Fig. 3b, spectrum I). Because of this, it appears to be impossible to reveal the difference in the state of carbon in the first layer before and after mixing by the XPS data, although the irradiation suggests disordering. In the transition layer of the sputtered carbon film, a state with the bond energy of the electrons at the C1s level of 282 eV is added to the three states of carbon atoms noted above (Fig. 3a, spectrum 2). This value of the bond energy can correspond to titanium carbide TiC [8]. This state
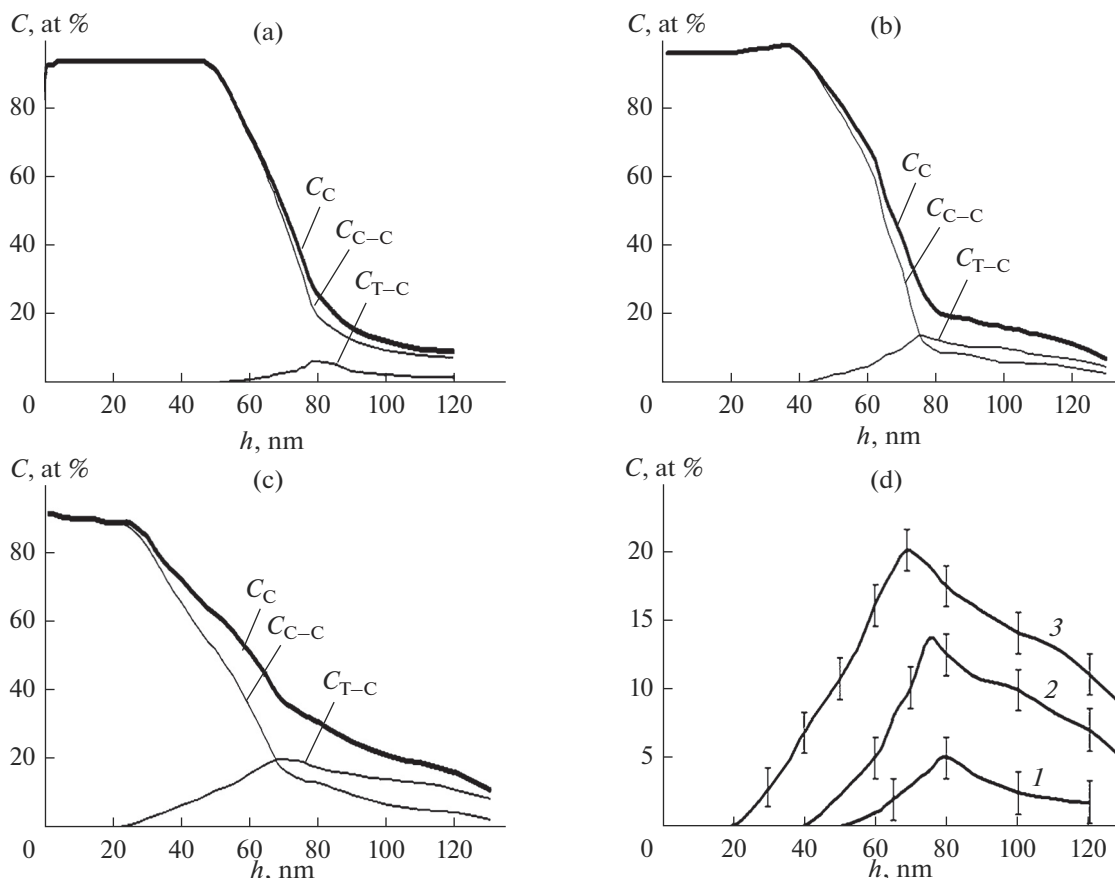
Fig. 4. (a–c) Concentration profiles of the distribution of carbon with C–C and Ti–C bonds: (a) in the initial film and (b, c) after ion beam mixing with Ar^+ ions with irradiation doses of (b) 10^{17} and (c) 4×10^{17} ion/cm^2; (d) concentration profiles of the distribution of carbon with Ti–C bonds: (*1*) in the initial film and after mixing at irradiation doses of (*2*) 10^{17} and (*3*) 4×10^{17} ion/cm^2.

of carbon atoms also manifests itself in the film after mixing, but the spectrum is more intense. This is evidence of the fact that the amount of titanium carbides TiC in the film after mixing is greater than in the initial film. In addition, there is carbon with the bond energy of 283.1 eV in the mixed film (Fig. 3b, spectrum *2*). The XPS spectrum for this form of carbon turns out to be shifted toward smaller bond energy relative to carbon with the sp^2 hybridization of the C–C bonds by 1.3 eV, which indicates a negative effective charge on the carbon atoms and, hence, suggests a bond between carbon and titanium. The negative effective charge on carbon atoms occurs owing to the decrease in the number of C–Ti bonds in favor of C–C bonds. This suggests that clusters of titanium carbides with an intermediate composition, e.g., titanocarbohedrene Ti_8C_{12} or titanium carbides with the nonstoichiometric ratio of the components, are present in the transition layer.

If the state of the carbon atoms in the C1s spectra is conditionally divided into two bands, the first of which corresponds to the Ti–C bonds and the second corresponds to the superposition of the state of carbon with C–C and C–O–H bonds but mainly with C–C

bonds, the concentration of carbon consumed for the formation of the Ti–C bonds can be qualitatively estimated. Such a calculation was performed in this work, and its results are reflected in Fig. 4. It is seen from Fig. 4 that the concentration of carbon in the transition layer of the initial film in the Ti–C bonds does not exceed 5 at % (Fig. 4a), while the concentration of carbon in the Ti–C bonds in the layers mixed with Ar^+ ions increases and reaches a value of 20 at % at the irradiation dose of 4×10^{17} ion/cm^2 (Fig. 4d, curve *3*). This directly indicates the formation of titanium carbides in the transition layer as a result of the ion beam mixing of the carbon film. Apparently, the formation of titanium carbides in the transition layer is one of the reasons for the increase in the microhardness of the samples after mixing.

The RS spectrum of the carbon film after sputtering is represented by two strongly diffuse bands D at $\Delta v \sim 1375$ cm^{-1} and G at $\Delta v \sim 1582$ cm^{-1} with the ratio of the intensities D/G $\sim$ 1 (Fig. 5). In addition, the spectrum is diffuse to the left of the D band to the region of low-frequency shifts. The position of the G peak depends on the structure of the material and
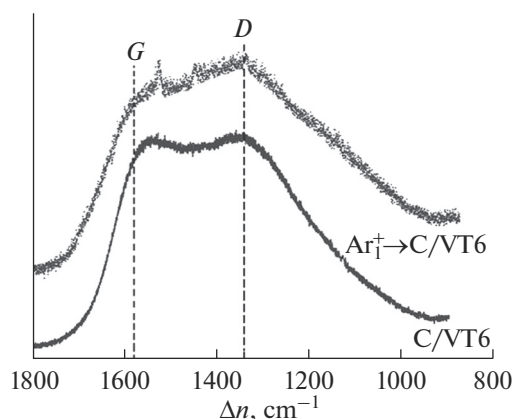
Fig. 5. Raman spectra of a carbon magnetron film on a titanium alloy (C/VT6) and a film irradiated with Ar^+ ions with $E = 30$ keV and $D = 10^{17}$ ion/cm^2 ($Ar_1^+ \rightarrow$ C/VT6).
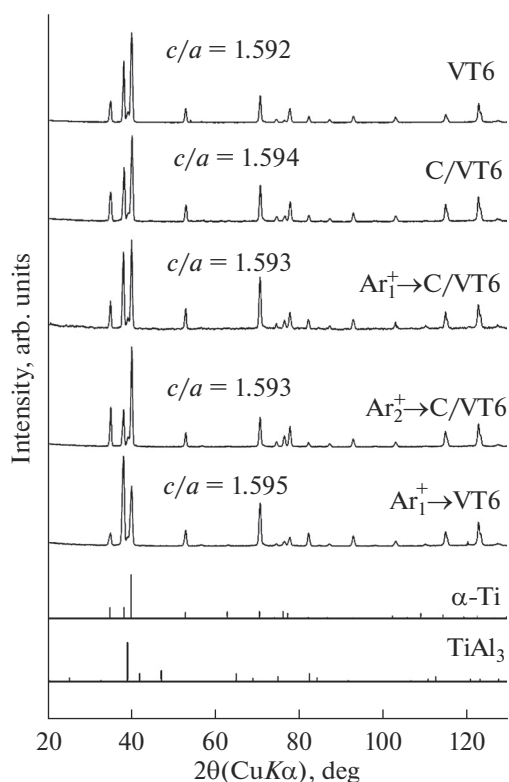

Fig. 6. Diffraction patterns of the samples of VT6 in the initial state (VT6), after sputtering of a carbon film (C/VT6), after mixing with irradiation doses of 10^{17} ($Ar_1^+ \rightarrow$ C/VT6) and 4×10^{17} ion/cm^2 ($Ar_2^+ \rightarrow$ C/VT6), and after irradiation with a dose of 10^{17} ion/cm^2 ($Ar_1^+ \rightarrow$ VT6). The error of determination of c/a is ± 0.002 Å.

increases in the case of transition from the structure of graphite to the nanocrystalline state [9]. The presence of the D band corresponds to the disordered state. It should be noted that a similar spectrum of the same film applied to a sitall plate is represented by more resolved D and G peaks. Because of this, there are grounds to assume that the weak dip between these peaks in the spectrum of the carbon film is partially associated with the formation of a band from Ti–C structures. Therefore, the carbon film consists of disordered, predominantly sp^2 hybridized carbon with an insignificant fraction of sp^3 carbon. Here, the strong overall diffusion of the spectrum can be associated with the high structural nonuniformity of the film along the depth of the layer under analysis as well as the formation of Ti–C structures. Ion bombardment (mixing) leads to a further substantial increase in the degree of disordering of the carbon layer (Fig. 5). The D and G bands are almost unresolved, the D/G ratio is higher than unity, and there is no dip between them. The intensity of the spectrum to the left of the D band increases. On the basis of these data, the formation of a disordered structure of a film of carbon that is predominantly in the sp^2 hybridized state, as well as the increase in the fraction of the structures of nonstoichiometric titanium carbides, can be stated.

The studies via X-ray phase analysis revealed that the phase composition of all the samples was mainly represented by α-Ti with a hexagonal close-packed (HCP) crystal lattice and an insignificant fraction (of no more than 5 wt %) of the phase of TiAl$_3$ (Fig. 6). The degree of tetragonality c/a of the HCP structure of α-Ti for the samples in the initial state is 1.592 Å and corresponds within the error of calculation (± 0.002 Å) to the degree of tetragonality of the samples after the sputtering of a carbon film and its ion beam mixing and after irradiation with Ar^+ ions.

However, the calculation of the coherent scattering regions (CSRs) revealed that, in cases where there is an ion beam action on the sample, with a carbon film or without it, a decrease in the CSR from 480 Å for the initial sample to 350–380 Å is observed (Table 2). This can occur in cases where dislocations appear in the grains, and the formation of dislocation structures occurs [10]. It is known [3] that a change in the defect structure and/or structural phase state in the layer located directly behind the surface layer, in which the slowdown of the ions being incorporated takes place, occurs in annealed metals with a low density of dislocations upon ion irradiation. It is conventional to call this effect an effect of long-range action. Upon the irradiation of annealed metals, the effect of long-range action manifests itself primarily in the increase in the density of dislocations by 1–1.5 orders of magnitude and formation of dislocation substructures. Because of this, it is assumed that the decrease in the CSR in the titanium alloy as a result of irradiation is a consequence of the manifestation of the effect of long-range action. However, the formation of titanium carbides and disordering of the carbon film rather than the change in the dislocation structure beyond the projective range of ions is determining in the increase in microhardness.

CONCLUSIONS

The formation of a disordered structure of carbon that is predominantly in the sp^2 hybridized state occurs as a result of ion beam mixing in the samples of VT6 titanium alloy.

Conditions for the formation of titanium carbides are generated in the transition region of the film/substrate system upon mixing. The formation of nonstoichiometric structures of titanium carbides as well as titanium carbide TiC is possible.

The formation of a disordered structure of carbon and titanium carbides determines an increase in the microhardness of the samples by 100% or more.

REFERENCES

1. Andrievski, R.A., Nanomaterials based on high-melting carbides, nitrides and borides, *Russ. Chem. Rev.*, 2005, vol. 74, no. 12, pp. 1061−1072.

2. Hauert, R. and Patscheilder, J., From alloing to nanocomposites−improved performance of hard coatings, *Adv. Eng. Mater.*, 2000, vol. 2, no. 5, pp. 247−259.

3. Kurzina, I.A., Kozlov, E.V., and Sharkeev, Yu.P., *Gradientnye poverkhnostnye sloi na osnove intermetallidnykh chastits* (Gradient Surface Layers Based on Intermetallic Particles), Tomsk: Izd. Nauchno-Tekh. Liter., 2013.

4. Kalin, B.A., Volkov, N.V., and Oleinikov, I.V., Ion mixing in multilayer films and the doping of the near-surface layers of polycrystalline substrates under irradiation by ion beams with a wide energy spectrum, *Bull. Russ. Acad. Sci.: Phys.*, 2012, vol. 76, no. 6, pp. 690−695.

5. Burenkov, A.F., Komarov, F.F., Kumakhov, M.A., and Temkin, M.M., *Tablitsa parametrov prostranstvennogo raspredeleniya ionno-implantirovannykh primesei* (Table of Parameters of Spatial Distribution of Ion-Implanted Impurities), Minsk: Bel. Gos. Univ., 1980.

6. D'yakonova, N.P., Shelekhov, E.V., Sviridova, T.A., and Reznikov, A.A., Quantitative x-ray phase analysis of weakly textured objects, *Zavod. Lab.*, *Diagn. Mater.*, 1997, vol. 63, no. 10, pp. 17−24.

7. Dorofeev, G.A., Povstugar, I.V., Protasov, A.V., Elsukov, E.P., and Streletskii, A.N., Determination of nanoparticle sizes by x-ray diffraction, *Colloid J.*, 2012, vol. 74, no. 6, pp. 675−685.

8. Wagner, C.D., Rigus, W.M., and Davis, L.E., *Handbook of X-Ray Photoelectron Spectroscopy*, Eden Prairie, MN: Perkin-Elmer, 1979.

9. Ferrari, A.C. and Robertson, J., Raman spectroscopy of amorphous, nanostructured, diamond-like carbon, and nanodiamond, *Philos. Trans. R. Soc., A*, 2004, vol. 362, pp. 2477−2512.

10. Gulyaev, A.P., *Metallovedenie* (Metal Science), Moscow: Metallurgiya, 1977.

Translated by E. Boltukhina

SPELL: 1. OK